PHYSICAL REVIEW B VOLUME 36, NUMBER 16 1 DECEMBER 1987

Temperature-dependent rare-earth impurity-site symmetries in CaF_2

T. Szczurek* and M. Schlesinger
Department of Physics, University of Windsor, Windsor, Ontario, Canada N9B 3P4

(Received 21 April 1987)

We present evidence for the existence of a new class of rare-earth impurity-site symmetries in CaF_2, sites whose characteristic spectrum does not exist or is much diminished below a given temperature.

I. INTRODUCTION

The vacuum ultraviolet absorption spectra of crystals doped with tripositive rare-earth ions (R^{3+}) are usually attributed to interconfigurational f-d transitions in these ions. The interconfigurational f-d transitions are easily distinguished from the intraconfigurational f-f transitions. The first are parity allowed, consequently, they give rise to high-intensity lines in the spectrum. The second are parity forbidden and it is only the crystal-field configurational mixing that makes them observable.

Many crystals may be doped with R^{3+} ions; however, in investigations concerning f-d transitions, calcium fluoride offers the widest spectral range, from about 400 cm^{-1} up to about 80 000 cm^{-1}.

Absorption spectra of CaF_2:R^{3+} crystals arising from f-d transitions in the R^+ ions are known[1] mainly from the investigations by Kaplyanski and co-workers and Loh in the sixties and by ourselves in the seventies.

In the present work we present some high-resolution absorption data for CaF_2:Tm^{3+} and CaF_2:Sm^{3+}. We focus our attention at temperature-dependent features in the spectra and propose the existence of a new class of impurity site symmetries.

The simultaneous presence of different impurity sites is to be expected.[2] What we postulate is the existence of sites whose spectra is much diminished *below* a given temperature.

II. EXPERIMENTAL PROCEDURE

Crystals used in this study were grown and supplied by Optovac, Inc. These were randomly oriented and were used as received except that samples of proper dimensions were prepared by either cleaving or cutting and subsequent polishing. Impurity concentration values are given in atomic percentage present in the growth melt.

Absorption measurements were carried out using our[3] double beam adaptor to the vacuum-ultraviolet (McPherson Model 225) spectrometer. In the spectrometer we used a grating with 1200 grooves per mm. Home built microwave driven Xe- or Kr-gas lamps served as a source of the vacuum-ultraviolet (VUV) radiation. The cryostat itself in which the crystals were held and which was mounted at the spectrometer's exit slit was specially designed for work at the full range between liquid helium and room temperatures. Temperature was monitored using a Ge thermometer. Temperatures between, say, liquid helium and liquid nitrogen were "fixed" by slow cooling ($\frac{1}{2}$ K/min) while each full run at a given temperature (see Fig. 2 for instance) took less than 10 min. In passing it should be stated that a slow warming "fixing" yielded identical results. The monochromatic VUV beam transmitted by the sample was detected by a solar-blind Hamamatsu Model R1460 photomultiplier. Due to its high sensitivity and the special grating, we were able to use slits as narrow as 10 μm and so a narrow instrumental spectral width was achieved.

III. RESULTS

In Fig. 1 we present the VUV absorption spectrum of a CaF_2:Tm^{3+} crystal with impurity concentration 0.05 at. % and of thickness 0.4 mm. Figure 1(a) is for the wavelength range 154–160 nm and Fig. 1(b) for the range 140–146 nm. Spectra were taken at liquid-helium temperature. We identify in the first curve four (B,C,D,E) zero-phonon absorption lines and their associated local phonon side bands at 494 cm^{-1} from their parent lines. The lines designated, $\overset{B}{1}$, $\overset{B}{2}$, and so on correspond to lattice phonons of the CaF_2 host associated with the strong B line. Such identification becomes possible as a result of the relatively high resolution grating used in these measurements. We have indicated in Fig. 1(a) the spectral location of line A^* which is a temperature-dependent zero-phonon feature. In Fig. 2(a) we present a family of curves taken at different temperatures (13–109 K) and corresponding to the spectral region of 158–160 nm. The curves depict the temperature-dependent intensity of the (A^*) line at 159.79 nm. Due to the line's intensity and relatively isolated position, three of its phonon side bands are also evident (at 88, 155, and 226 cm^{-1} from the parent feature). Figure 2(b) is similarly showing the temperature dependency of the line at 145.26 whose spectral position is indicated (F^*) on the spectrum of Fig. 1(b). It must be emphasized that the curves in both Figs. 2(a) and 2(b) were obtained when a series of measurements was made while crystal temperature was slowly falling. There was no effect upon the results even after a large number of temperature cycles.

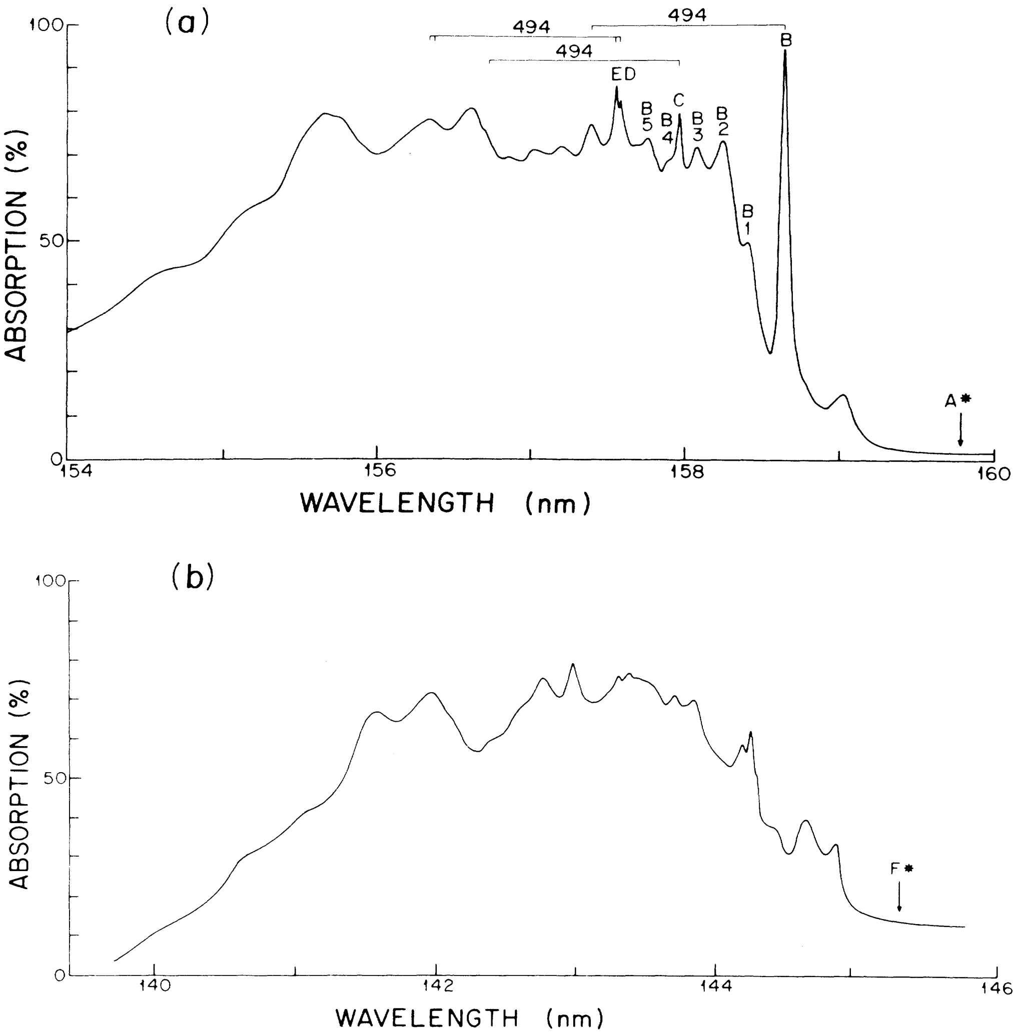

FIG. 1. Vacuum ultraviolet absorption spectrum of a 0.4-mm-thick CaF_2:Tm^{3+} crystal with impurity concentration 0.05 at. %. (a) Wavelength range of 154–160 nm. (b) Wavelength range of 140–146 nm, spectra taken at liquid-helium temperature.

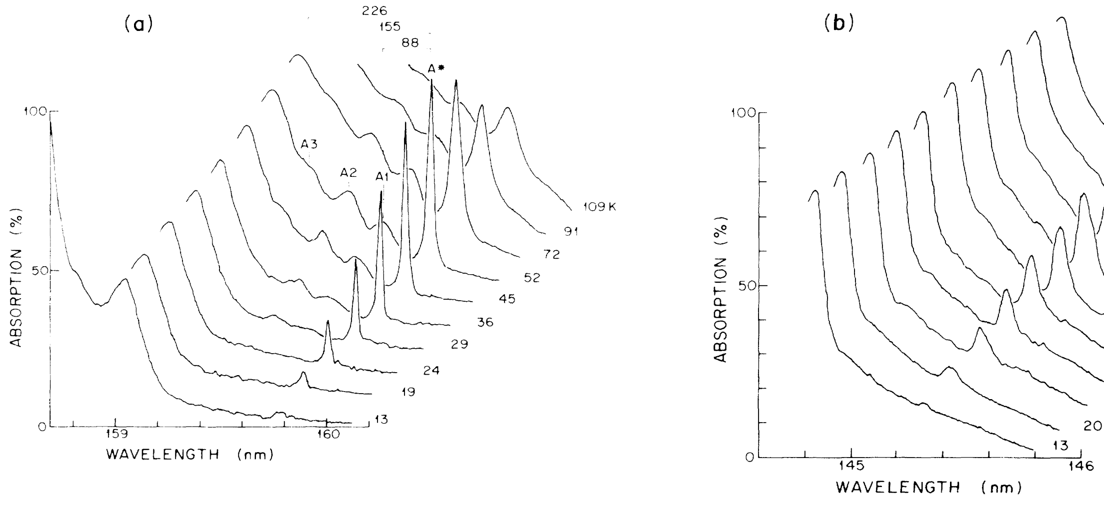

FIG. 2. Families of curves showing temperature-dependent absorption for the same crystal as in Fig. 1. (a) Wavelength range of 158–160 nm. (b) Wavelength range of 145–146 nm.

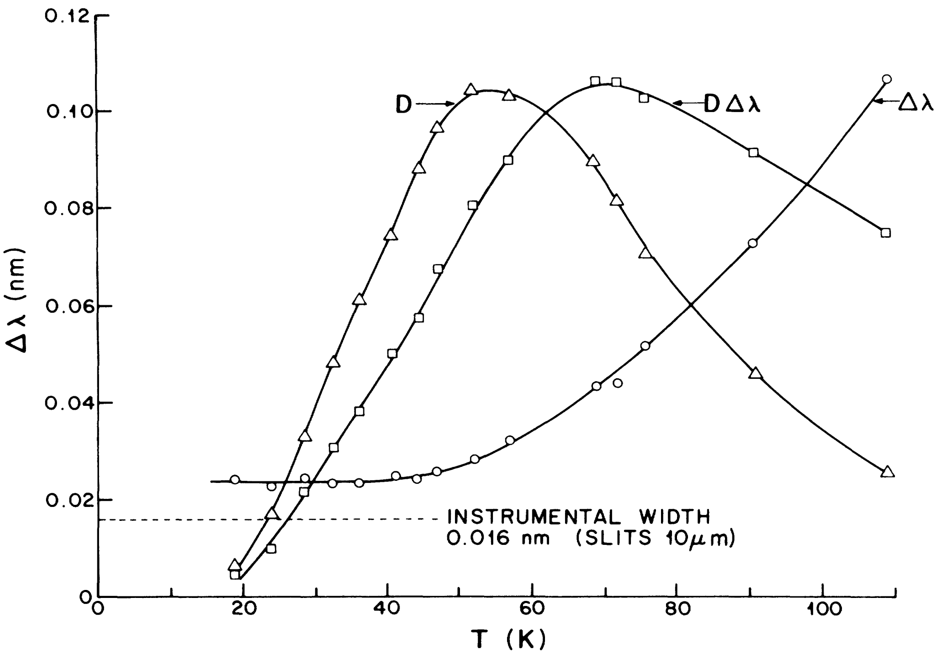

FIG. 3. The optical density at peak absorbance (D), the width at half peak ($\Delta\lambda$), and the product ($\Delta\lambda D$) for the feature A^* in Fig. 2(a).

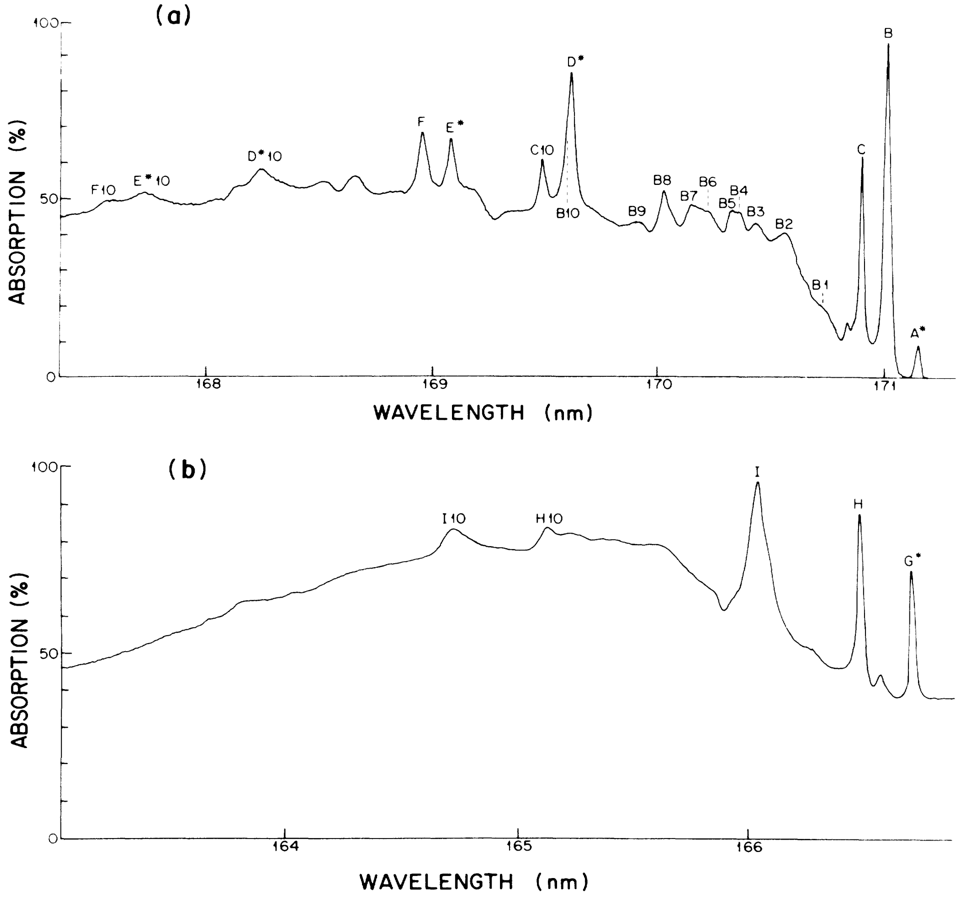

FIG. 4. Vacuum ultraviolet absorption spectrum of a 1.6-mm-thick CaF_2:Sm^{3+} crystal with impurity concentration of 0.005%. (a) Wavelength range of 167–171 nm. (b) Wavelength range of 163–167 nm, spectra taken at 60 K.

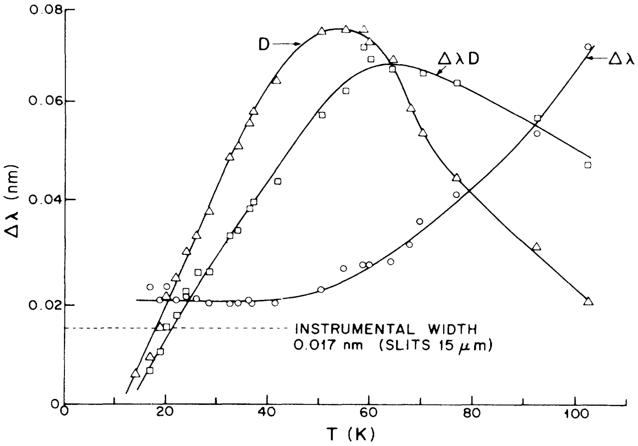

FIG. 5. The optical density at peak absorbance (D), the width at half peak ($\Delta\lambda$), and the product ($\Delta\lambda D$) for the feature G^* in Fig. 4(b), as a function of temperature.

In Fig. 3 we present the optical density at peak absorbance (D), the optical width at half absorbance ($\Delta\lambda$), and the product of the two ($D\Delta\lambda$) as a function of temperature for the feature A^*. The instrumental spectral width is also indicated on the figure for comparison. Similar behavior is exhibited by feature F^* as well.

In Fig. 4 the absorption spectrum of CaF_2:Sm^{3+} crystal with impurity concentration 0.005 at. % and thickness 1.6 mm is given. Spectrum was taken at about 60 K (solid-N_2 temperature). This was so chosen since all lines designated as "temperature dependent" and labeled with an asterisk are found to be at their maximum intensity at around this temperature. Figure 4(a) illustrates the spectral region of 167–171 nm and Fig. 4(b) the region of 163–167 nm. As a typical example, we present in Fig. 5 the same data as in Fig. 3, but for the feature at 166.70 nm [G^* in Fig. 4(b)]. In Table I we summarize wavelength, etc., of zero-phonon lines and associated vibronics corresponding to curves in Figs. 1 and 4.

In summary, all features designated by an asterisk do not survive at liquid-helium temperature and below or at about 120 K and above. The same is true regarding their associated vibronics. In fact, it is noted that their temperature-dependent characteristics are well represented by either Figs. 3 or 5.

IV. DISCUSSION

As in previous cases,[4,5] the spectra presented in Fig. 1 are due to $4f^{12}$-$4f^{11}5d$ transitions of the Tm^{3+} ion in CaF_2. In particular, Fig. 1(a) is to be compared with Fig. 3(a) in Ref. 4. The resolution (about 1 cm^{-1}) in the present spectra is, however, improved by about a factor of 10 as can be noted by observing the separation between peaks E and D [Fig. 1(a)] which are not resolved in the previous case. Special attention is to be paid to A^* and F^* which at liquid-helium temperature are completely absent and whose temperature-dependent behavior is presented in Figs. 2(a) and 2(b), respectively. To further clarify and quantify the thermal behavior of A^*, Fig. 3 presents data pertaining to its optical density at peak value and half-width at half-peak value. Shown is also the product of D and $\Delta\lambda$ as a function of temperature. In Fig. 5 similar data for the G^* feature in the absorption spectrum of CaF_2:Sm^{3+} is depicted and a similar behavior is observed.

One might be tempted[1] to interpret these spectral lines as originating from thermally excited Stark levels of the initial $4f^{11}$ configuration ("hot" lines). The kT value for the temperature range of 60–70 K is about 50 cm^{-1}. The separation (see Table I) between lines A^* and B for the case of Sm^{3+} is 46 cm^{-1} and the separation between the lines E^* and F is also 46 cm^{-1}. These values are in agreement with the "hot" line interpretation. For the case of the Tm^{3+} ion, the "hot" line interpretation will not be possible since the separation between lines A^*

TABLE I. Zero-phonon lines and vibronics in absorption spectra of CaF_2:Tm^{3+} and CaF_2:Sm^{3+} (see Figs. 1 and 4).

Impurity	Zero-phonon line	λ (nm)	υ (cm^{-1})	Identifiable vibronics (in cm^{-1} from zero-phonon line) 1	2	3	4	5	6	7	8	9	10
Tm^{3+}	A^*	159.79	62 582	88	155	226							
	B	158.65	63 032	95	151	221	230	343					494
	C	157.97	63 303										494
	D^*	157.60	63 452										
													494
	E	157.56	63 468										
	F^*	146.65	68 190										
Sm^{3+}	A^*	171.158	58 426										
	B	171.022	58 472	98	160	195	218	231	266	296	336	375	484
	C	170.910	58 510										484
	D^*	169.640	58 948										485
	E^*	169.106	59 135										481
	F	168.972	59 181										483
	G^*	166.707	59 985										
	H	166.500	60 060										487
	I	166.055	60 221										481

and B is 550 cm^{-1}, while between D^* and E it is 16 cm^{-1}.

The other interpretation is that of temperature-dependent site symmetries. Due to the close resemblance of the data in Figs. 3 and 5, it is reasonable to offer an identical interpretation to the cases of Tm^{3+} and Sm^{3+}.

Temperature dependent site symmetries of Tm^{3+} in SrF_2 were reported[5] by us recently. These were sites of a new class, i.e., sites whose characteristic spectrum does not exist or is much diminished *below* a given temperature. The spectra reported in Ref. 5 were those originating from infrared excited f^n energy states, whereas here we are dealing with excitation from ground multiplets in either Tm^{3+} or Sm^{3+}.

The identity and nature of the sites might not be the same for the two impurities and/or the two hosts. The significant issue is the fact that the sites seem to exist only in a relatively narrow range of temperatures. This may come about, for instance, by charge compensating F^- or O^{2-} ions hopping between two positions. At a sufficiently low temperature the contraction of the lattice freezes out one of the two possible sites. The curves describing $\Delta\lambda D$ can be viewed as a measure of the number of sites responsible for the temperature-dependent absorption features (Figs. 3 and 5). Note, however, that D and, therefore, $D\Delta\lambda$, are in arbitrary units in Figs. 3 and 5.

Clearly, more experimental work would be required to quantitatively establish the nature of these "new" sites. It is noteworthy that however different the temperature-dependent site may be from any other, they too exhibit phonon side bands whose displacement from the parent line is about 480 cm^{-1}. This site-symmetry independence[6] of the local phonon frequency is an additional indication of it being the highly symmetrical breathing mode of the eight nearest-neighbor fluorines. It is from these, in any case, where the largest contribution to the crystal field to which the impurity ions are subject comes from.

ACKNOWLEDGMENT

Support by the Natural Sciences and Engineering Research Council of Canada is gratefully acknowledged.

---

[*] Permanent address: Institute of Physics, Nicholas Copernicus University, ul. Grudziadzka 5, 87-100 Torun, Poland.

[1] See, for instance, T. Szczurek and M. Schlesinger, in *First International Symposium on Rare Earth Spectroscopy,* edited by B. Jezowska, J. Legendziewicz, and W. Strek (World Scientific, Singapore, 1985), pp. 309–330, and many references therein.

[2] M. P. Miller and J. C. Wright, J. Chem. Phys. **71**, 324 (1979).

[3] M. Schlesinger and T. Szczurek, Rev. Sci. Instrum. **44**, 1720 (1973).

[4] T. Szczurek and M. Schlesinger, Phys. Rev. B **34**, 6109 (1986).

[5] M. Schlesinger and T. Szczurek, Phys. Rev. B **35**, 8341 (1987).

[6] M. Schlesinger and G. W. F. Drake, Can. J. Phys. **54**, 1699 (1976).